

# ASSESSMENT OF CAPABILITIES OF LIDAR SYSTEMS IN DAY- AND NIGHT- TIME UNDER DIFFERENT ATMOSPHERIC AND INTERNAL-NOISE CONDITIONS

Ravil Agishev<sup>1</sup>, Adolfo Comerón<sup>2</sup>

<sup>1</sup> Kazan State Power Engineering University, 51, Krasnoselskaya St., Kazan 420066, Russia

<sup>2</sup> Universitat Politècnica de Catalunya, Jordi Girona 1-3, 08034 Barcelona, Spain

## ABSTRACT

As an application of the dimensionless parameterization concept proposed earlier for the characterization of lidar systems, the universal assessment of lidar capabilities in day and night conditions is considered. The dimensionless parameters encapsulate the atmospheric conditions, the lidar optical and optoelectronic characteristics, including the photodetector internal noise, and the sky background radiation. Approaches to ensure immunity of the lidar system to external background radiation are discussed.

## 1 INTRODUCTION

When conducting atmospheric measurements, the echo signals carrying information about the medium properties are received in presence of sky background radiance [1-4]. The signal-to-noise ratio (SNR)  $\rho$  of the generalized lidar system of direct photodetection with internal amplification in presence of internal noise and external background radiation can be written as follows [1-3]

$$\rho = \sqrt{N} \cdot P_s / \sqrt{P_q(P_s + P_b) + P_n^2} \quad (1)$$

where  $P_s$  and  $P_b$  are respectively the signal and background powers reaching the photodetector,  $P_q = 2 \cdot h \cdot c \cdot F \cdot \Delta f / \eta \cdot \lambda$ , with  $h$  the Planck's constant,  $c$  the speed of light,  $F$  the photodetector excess noise factor,  $\Delta f$  the photoreceiver electrical bandwidth,  $\eta$  the photodetector quantum efficiency, and  $\lambda$  the wavelength, and  $P_n = NEP \cdot \Delta f^{1/2}$ ;  $N$  is the number of accumulation cycles.

Our aim in the application and promotion of the methodology of dimensionless parametric modeling of lidar systems [5-8] is to show how the sensitivities of lidars using different types of photoreceivers with different noise parameters are impaired under the background of daytime sky and the variability and interdependent effects of atmospheric optical conditions, as well as to illustrate the practical possibilities for efficient and fair visual comparison of different lidars.

## 2 METHODOLOGY

The dimensionless parametric methodology of analysis and comprehensive comparison of lidar systems [5-7], including generalization, modification and simplification of traditionally used algorithms to assess the SNR and measurement accuracy, facilitates a quantitative comparison of different lidars.

Following this approach, we introduce a reference echo-signal  $P_{s0}$  as the signal that would attain the lidar photodetector from the reference range  $R_0$  in a standard reference molecular atmosphere. We also introduce a reference background power  $P_{b0}$  on the photodetector. The application of algorithms [8] normalizing the individual SNR components of (1) to the reference echo signal and comparing normalized system noises and atmosphere conditions refines the approach of the methodology presented in [5-7].

### 2.1 Partial SNRs and degrees of quantum noise exceeding

The normalized lidar signal  $P_s/P_{s0}$  can be presented as follows [5-7]:

$$\Pi \equiv P_s/P_{s0} = Q \cdot W^2 \cdot r^{-2}, \quad (3)$$

where for aerosol backscattering lidar:

$$Q = \frac{\beta_\pi(\lambda, R)}{\beta_{0\pi}(\lambda, R_0)} \quad W = \frac{T(\lambda, \alpha, R)}{T(\lambda, \alpha_0, R_0)} \quad r = R/R_0, \quad (4)$$

$\beta_\pi(\lambda, R)$  and  $\beta_{0\pi}(\lambda, R_0)$  being the backscatter coefficient at the  $\lambda$  wavelength at respectively the range  $R$  in the actual conditions and at the reference range  $R_0$  in the reference atmosphere. Likewise  $T(\lambda, \alpha, R)$  and  $T(\lambda, \alpha_0, R_0)$  are the atmospheric transmittances from the lidar respectively to range  $R$  in actual conditions and to range  $R_0$  in the reference atmosphere. We will use the partial signal-to-noise ratios  $S_q$ ,  $S_{b0}$ ,  $S_n$  as specific indicators of potentialities and sensitivity decreasing of lidar sounding with respect to the reference atmosphere. The sensitivity reductions are caused by shot noise of signal and background clutter and by internal noise of the photodetector:

$$S_q = P_{s0}/P_q; \quad S_n = P_{s0}/P_n; \quad S_{b0} = P_{s0}/P_{b0} \quad (5)$$

The emphasis on the partial relations  $S_q$ ,  $S_n$ ,  $S_{b0}$  and the  $\Pi$ -parameter allows to consider different sources of internal and external noise inherent to a particular system, and to associate them with parameters of the sounded media [8]. In this case, the system noises and their influences can be considered not "in themselves" and independently, but in comparison with the reference echo-signal from the reference range, which is formed as a result of sounding the reference atmosphere by particular/concrete lidar system under the background radiation of the reference brightness.

Equation (1) can be rewritten using the normalized echo-signal of Eq. (3) and the partial SNRs  $S_q$ ,  $S_{b0}$ ,  $S_n$  of Eq. (5) [8]:

$$\rho = \frac{\sqrt{N} \cdot \Pi}{\sqrt{S_q^{-1} \cdot (\Pi + b_{rel}/S_{b0}) + S_n^{-2}}} \quad (6)$$

where the relative background brightness  $b_{rel} = B_\lambda/B_{0\lambda}$  is the ratio of the actual sky brightness  $B_\lambda$  and the reference one  $B_{0\lambda}$ .

We'll use the generalized A-parameter [8] as a dimensionless characteristic of the lidar noises in presence of background radiation:

$$A = S_q/S_n^2 + b_{rel}/S_{b0} \quad (7)$$

Then the lidar SNR can be written as [8]:

$$\rho = \frac{\Pi \cdot \sqrt{N} \cdot \sqrt{S_q}}{\sqrt{\Pi + A}} = \sqrt{N \cdot \Pi \cdot S_q} \cdot \sqrt{\frac{\Pi}{\Pi + A}} \quad (8)$$

and it can be applied to any lidar instrument.

When sounding the night sky at the background brightness being considered minimal, i.e. when the ratio of the "current" to night sky background brightness  $b_{rel}=B_\lambda/B_{0\lambda}=1$ , it is useful [8] to select an important component  $A_0$  within the A-parameter,

$$A_0 = S_q/S_n^2 + S_{b0}^{-1} \quad (9)$$

since  $A = A_0 + (b_{rel} - 1)/S_{b0}$  (10)

It should be underlined, that taking into account  $S_{b0}^{-1}$  along with  $S_q/S_n^2$  is especially important, when using photodetectors with low level of dark current.

## 2.2 $L_0$ as potentialities prediction parameter

Following Eq. (8), the dimensionless system parameter  $L_0$  [8], defined as the SNR achieved by sounding the reference atmosphere at the reference range at reference night-sky background without accumulation ( $N=1$ ) is:

$$L_0 \equiv \rho(\Pi = 1, b_{rel} = 1, N = 1) = \sqrt{S_q/(1 + A_0)} \quad (11)$$

Thus the  $L_0$ -parameter in advance gives a forecast for the particular/concrete lidar's SNR, when receiving the echo-signal from the reference range of the standard molecular atmosphere. By setting the  $L_0$ -parameter as combination of the partial SNRs of various natures, which characterize the system noises of a specific lidar, one can evaluate the potentialities and compare different lidar systems at the preliminary stage, even before the remote measurements.

## 2.3 Lidar excess noise factor introduction

The last multiplier of (8) is a factor of SNR reduction by excess noise  $\Phi_{ex}$  [8], which caused by the detector's excess noise and the background radiation

$$\Phi_{ex} = \sqrt{\frac{\Pi}{\Pi + A}} = (1 + A/\Pi)^{-1/2}, \quad (12)$$

and indicates that the decrease of system capabilities can be caused by the interrelated influence of parameters of lidar system noises, background light and sounded medium.

## 2.4 Block diagram of system parameters' formation and interrelations

As follows from (8), (11) and (12), the system SNR for number of accumulation cycles  $N=1$  is

$$\rho = \Pi \cdot L_0 \cdot \sqrt{\frac{1 + A_0}{\Pi + A}}, \text{ or } \rho = \sqrt{\Pi \cdot S_q} \cdot \Phi_{ex} \quad (13)$$

when remembering that  $\Pi = Q \cdot W^2 \cdot r^{-2}$ . Therefore, both forms of expression (13) are represented as the product of dimensionless factors having their own nature.

Fig.1 represents a block diagram of the model with relationships between normalized system parameters  $S_q$ ,  $S_n$ ,  $S_b$ ,  $A$ ,  $A_0$ ,  $L_0$ ,  $\Phi_{ex}$ ,  $\Pi$  and  $b_{rel}$ , which determine the system potentialities  $\rho$ .

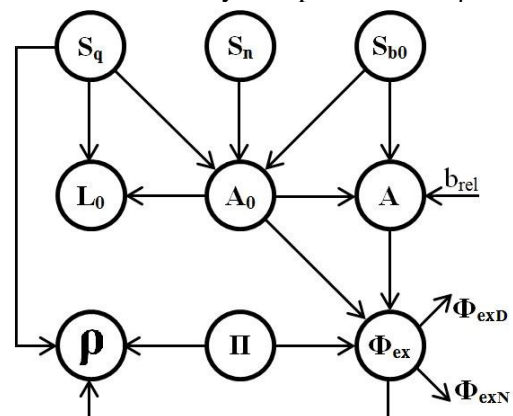


Fig. 1. Lidar modeling: Block diagram of relationships between system parameters.

### 3 RESULTS

#### 3.1 Degree of SNR reduction in day-time

In order to assess the lidar system capabilities under different atmospheric and internal-noise conditions, let's estimate the extent  $\Phi$  of the SNR decrease when sounding in day- and night- time:

$$\Phi = \frac{\Phi_{\text{exD}}}{\Phi_{\text{exN}}} \equiv \frac{\Phi_{\text{ex}}(b_{\text{rel}})}{\Phi_{\text{ex}}(b_{\text{rel}}=1)} = \sqrt{\frac{\Pi+A_0}{\Pi+A}} \quad (14)$$

Fig. 2 shows the extent to which the potentialities of lidar in day-time compared to night-time can decrease by representing  $\Phi = \Phi_{\text{exD}}/\Phi_{\text{exN}}$  as a function of the ratio  $A/A_0 = 1 + (b_{\text{rel}} - 1)/S_{b0}$  for a wide range of optical and physical sensing conditions ( $\Pi = 10^{-2} \dots 2 \cdot 10^2$ ) and noise properties of photodetectors ( $A_0 = 10^{-2} \dots 10^1$ ) (see also Table 1).

Table 1. System parameters considered.

SYSTEM PARA- METERS	RANGE of CHANGES		CALCU- LATIONS	RANGE of CHANGES			
	min	max		absolute		moderate/ reasonable	
				min	max	min	max
$P_{s0}, W$	$3 \cdot 10^{-9}$	$3 \cdot 10^{-5}$	$S_q$	3	$3 \cdot 10^6$	10	$10^5$
$P_q, W$	$10^{-11}$	$10^{-9}$	$S_n$	1	$3 \cdot 10^7$	10	$10^6$
$P_n, W$	$10^{-12}$	$3 \cdot 10^{-9}$	$S_{b0}$	30	$3 \cdot 10^7$	1	$10^4$
$P_{b0}, W$	$10^{-12}$	$10^{-10}$	$S_q/S_n^2$	$10^{-10}$	300	$10^{-3}$	300
$b_{\text{rel}}$	1	300	$A_0$	$3 \cdot 10^{-8}$	300	$10^{-4}$	100
$\Pi$	$10^{-6}$	$10^3$	$L_0$	$10^{-1}$	$2 \cdot 10^3$	1	200

The 3-D-graphs of Fig. 2 illustrate the degree of SNR reduction for low-noise photodetectors with  $A_0 \ll 1$  (a), for detectors with  $A_0 \sim 1$  (b) and for "noisy" detectors with  $A_0 \gg 1$  (c).

Fig. 2 illustrates the fact that the impact of the detector's internal noise and of the background radiation are not absolute, but they depend on the optical and physical properties of the sounded atmosphere, combined into the  $\Pi$ -parameter.

#### 3.3 Real lidar systems comparison

Results of the comparison of lidars A and B [9,10] are represented in Fig. 3. Their dimensionless parameters calculated are given in Table 2.

Table 2. Modeling parameters of Lidars A and B.

Modeling parameters	$S_q$	$S_n$	$S_{b0}$	$A_0$	$L_0$
Lidar A	$9.7 \cdot 10^3$	$1.5 \cdot 10^3$	$1.8 \cdot 10^3$	$5 \cdot 10^{-3}$	98.4
Lidar B	$4.0 \cdot 10^2$	$4.3 \cdot 10^4$	$3.5 \cdot 10^4$	$3 \cdot 10^{-5}$	20.1

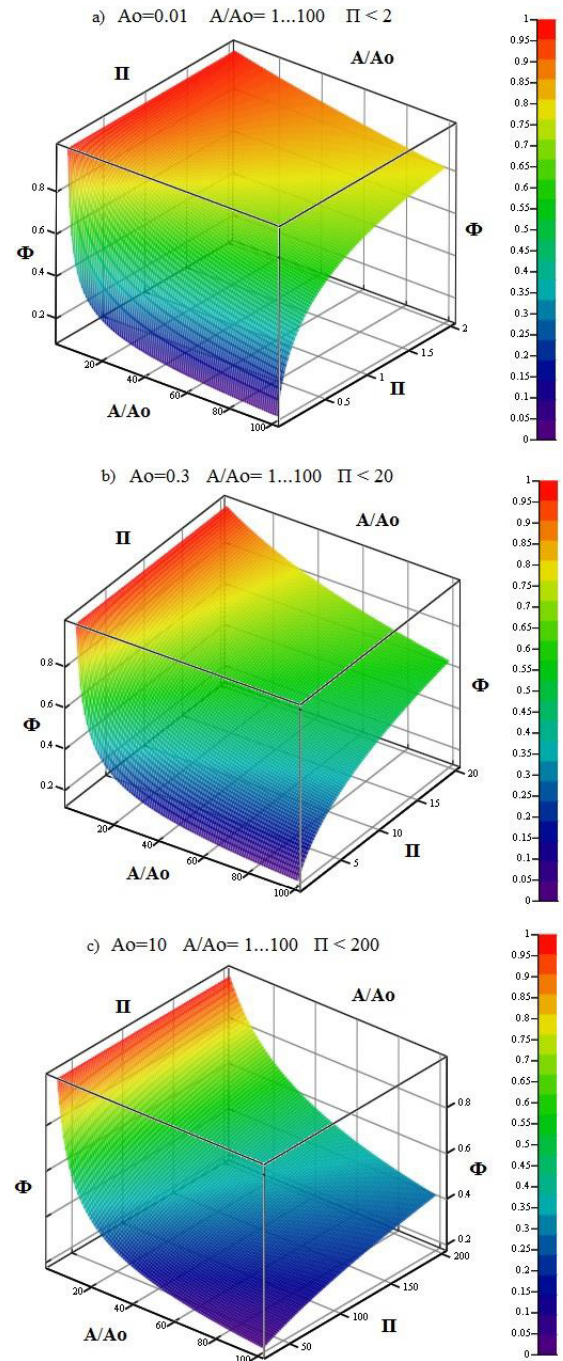
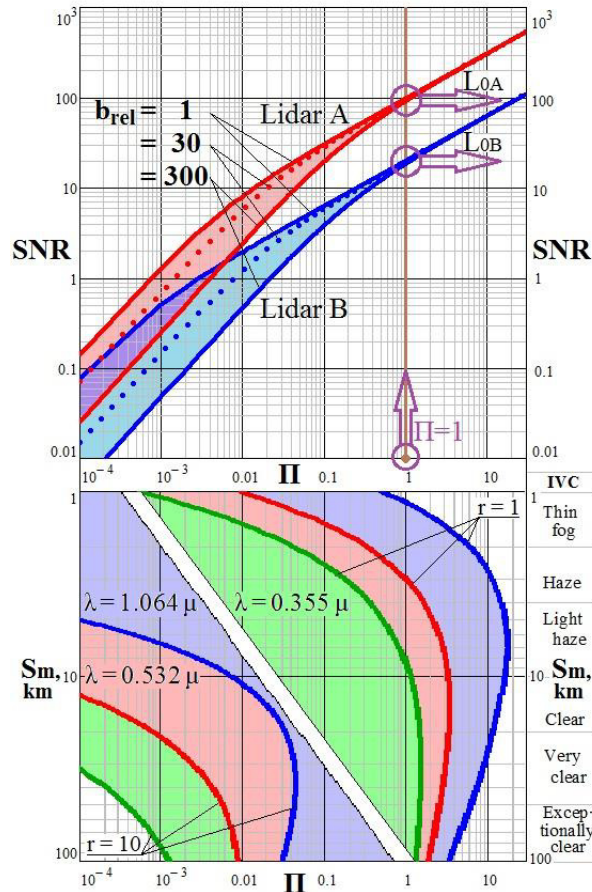


Fig. 2. The degree of SNR reduction as a function of the background noise intensity  $A/A_0$ , at wide variations of the normalized echo signal:  $\Pi = 10^{-2} \dots 2 \cdot 10^2$ , and the photodetector's excess noise:  $A_0 = 10^{-2}$  (a),  $A_0 = 0.3$  (b),  $A_0 = 10$  (c).

The generalized parameters  $L_{0A}$  and  $L_{0B}$ , which predict the potentialities of lidars at sounding the reference medium, are determined at  $\Pi=1$ . The

values  $b_{rel}=1, 30$  and  $300$  correspond to results of A and B lidars simulation, when sounding the atmosphere at weak, average and bright sky background under wide variations of its optical and physical parameters ( $\Pi = var$ ).



*Fig. 3. Comparison of A and B lidars potentialities on the “map”  $SNR = f(\Pi)$ . Lidars are considered sounding the same atmosphere for different values of the background noise brightness. Here:  $S_m$  is the visibility, km; IVC is the International Visibility Code.*

The generalized parameters  $L_{0A}$  and  $L_{0B}$ , which predict the potentialities of lidars at sounding the reference medium, are determined at  $\Pi=1$ . The values  $b_{rel}=1, 30$  and  $300$  correspond to results of A and B lidars simulation, when sounding the atmosphere at weak, average and bright sky background under wide variations of its optical and physical parameters ( $\Pi = var$ ).

As it can be seen from Fig. 3, the lidar A has the greater potentialities compared to the lidar B ( $L_{0A} \approx 100$ ;  $L_{0B} \approx 20$ ). It is seen that in day-time, when

working under intense sky background (e.g.  $b_{rel} = 300$ ), the A-lidar is able to receive approx. 10 times weaker echo-signals than B-lidar with a given accuracy (e.g.  $SNR=10$ ).

### References

- [1] Rees W. Physical Principles of Remote Sensing / Cambridge University Press, 2012. – 470 p.
- [2] Osche G. Optical Detection Theory for Laser Applications / New York, Wiley, 2011. - 442 p.
- [3] Kovalev V., Eichinger W. Elastic Lidar: Theory, Practice, and Analysis Methods / New York, Wiley-Interscience, 2004. – 615 p.
- [4] Saleh B., Teich M. Fundamentals of Photonics / New York, Wiley, 2011. - 965 p.
- [5] Agishev R., Comeron A., Gross B., Gilerson A. et al. Application of the method of decomposition of lidar signal-to-noise ratio to the assessment of laser instruments for gaseous pollution detection / *Applied Physics B*, 2004, vol. 79, No. 2, 255–264.
- [6] Agishev R., Comeron A., Rodriguez A. et al. Dimensionless parameterization of Lidar for laser remote sensing of the atmosphere and its application to systems with SiPM and PMT detectors / *Applied Optics*, 2014, vol. 53, No. 12, pp. 3164-3175.
- [7] Agishev R. Lidar Monitoring of the Atmosphere / Moscow, Phys-Math-Literature Press, 2009. - 316 p.
- [8] Agishev R. Potentialities of laser remote sensing systems of atmosphere monitoring at wide variability of optical physical characteristics / *Quantum Electronics*, 2017, vol. 47, No. 2, pp.140-152.
- [9] Comeron A., Agishev R. Dimensionless parameters for lidar performance characterization / in: Remote Sensing of Clouds and the Atmosphere // *Proceedings of SPIE*, 2014, vol. 9242, pp. 1-10.
- [10] Agishev R., Comeron A., Gilerson A. About the potential of LIDARs with different photodetectors under daytime sky radiation / *European Physical Journal: Laser Radar series*, 2016, vol. 119, pp. 2509-2513.